DOI: 10.1002/adma.200703008

Synthesis of Light-Diffracting Assemblies from Microspheres and Nanoparticles in Droplets on a Superhydrophobic Surface**

By *Vinayak Rastogi, Sonia Melle, Oscar G. Calderón, Antonio A. García, Manuel Marquez,* and *Orlin D. Velev**

Self-assembly of colloidal particles into crystalline arrays can be an effective tool for fabricating novel materials with advanced functionality. The periodicity at the micrometer and sub-micrometer length scales imparts light manipulation capability to these artificial structures in a manner similar to that in natural opals. Properties such as long-range ordering, maximal packing density, well-defined pore size, and high surface-to-volume ratio make these assemblies usable in areas such as photonics,[1–13] optical diffraction[14–16], antireflective coatings,[2,17–20] sensing,[21,22] separation processes, catalysis,[23,24] and anisotropic particle fabrication.[25]

Several methods have been devised to arrange organic or inorganic particles into well-ordered arrays.[26] Some techniques assemble the colloidal particles into macroscopic spherical structures that can encapsulate proteins, cells, food flavors, drugs, and other functional components. Such structures have been named colloidosomes, supraparticles, or supraballs.[27–29] The techniques for preparing supraparticles from monodisperse particle suspensions can be classified into two broad categories: Wet self-assembly (WSA) and dry self-assembly (DSA). WSA forms supraparticles by assembly inside or around droplet templates suspended in liquid media.[27,29–34] Examples of WSA include adsorption of particles on two-phase interfaces of emulsion droplets,[27,29,31–33,35,36] evaporation of floating colloidal suspension droplets,[29] or organization of particles with the assistance of microwaves.[37] WSA is problematic with regard to the subsequent use of the assembled structures because of the need to extract them out of the liquid medium which may be water or oil. The drying of the oil trapped inside the supraparticle pores slows down the process and may pose environmental problems. WSA does not allow robust control over the final shape of the supraparticles.

DSA encompasses methods for fabricating supraparticles using droplet templates dispensed on solid substrates. The oil-removal step is avoided and the assembled structures can be easily collected without further processing. The drying of the droplet leads to colloidal crystal formation by slowly restricting the thermal motion of particles through reduction of free volume.[38–40] The shape of the dried colloidal crystal depends on the wettability of the substrate. Park et al. have developed a DSA technique to create an array of hemispherical colloidal crystals using an ink-jet printing method.[38] Kuncicky et al. have shown that both the contact angle of the surface and the initial particle concentrations play important roles in determining the shape of colloidal assemblies.[39,40]

We report here a technique for colloidal assembly in droplets that reside on superhydrophobic substrates, which yields better control over the final shape and creates supraparticles that are easily detached and ready-to-use. The results of this process are near-spherical and spheroidal supraballs in dry environments. Droplets of 5.0 μL from a concentrated suspension of latex particles are dispensed on a superhydrophobic substrate coated with low-density polyethylene (LDPE).[41] LDPE was chosen because it is flexible, naturally hydrophobic, and inexpensive. The surfaces were generated by coating LDPE sheets with a solution of LDPE pellets in a mixture of xylene and methyl ethyl ketone (solvent and non-solvent, respectively). The purpose of the non-solvent is to increase the roughness and contact angle of the substrates. The LDPE substrate contact angles were in the range of 140°–150°. This enabled aqueous suspension droplets to assume a near-spherical shape, which led to the macroscopic casting of colloidal crystals (Fig. 1). We also used silicon nanowire (Si-NW)-coated superhydrophobic substrates,[41] which had contact angles higher than 170° and virtually no contact angle hysteresis.

[*] Prof. O. D. Velev, V. Rastogi
Department of Chemical and Biomolecular Engineering
North Carolina State University
Raleigh, NC 27695-7905 (USA)
E-mail: odvelev@unity.ncsu.edu
Prof. S. Melle, Prof. O. G. Calderón
Optics Department, School of Optics
Universidad Complutense de Madrid
Arcos de Jalón s/n – 28037 Madrid (Spain)
Prof. A. A. García, Prof. M. Marquez
Harrington Department of Bioengineering
Arizona State University
Tempe, AZ 85287 (USA)
Prof. M. Marquez
NIST Center for Theoretical and Computational Nanosciences
Gaithersburg, MD 20899 (USA)
Prof. M. Marquez
Center for Integrated Nanotechnologies
Los Alamos National Laboratory
Los Alamos, NM 87545 (USA)

[**] This research was supported by the Interdisciplinary Network of Emerging Science and Technology (INEST). We gratefully acknowledge John Schneider (ASU) for preparing superhydrophobic substrates and Dr. Chuck Mooney (AIF, NCSU) for SEM imaging.

ADVANCED MATERIALS

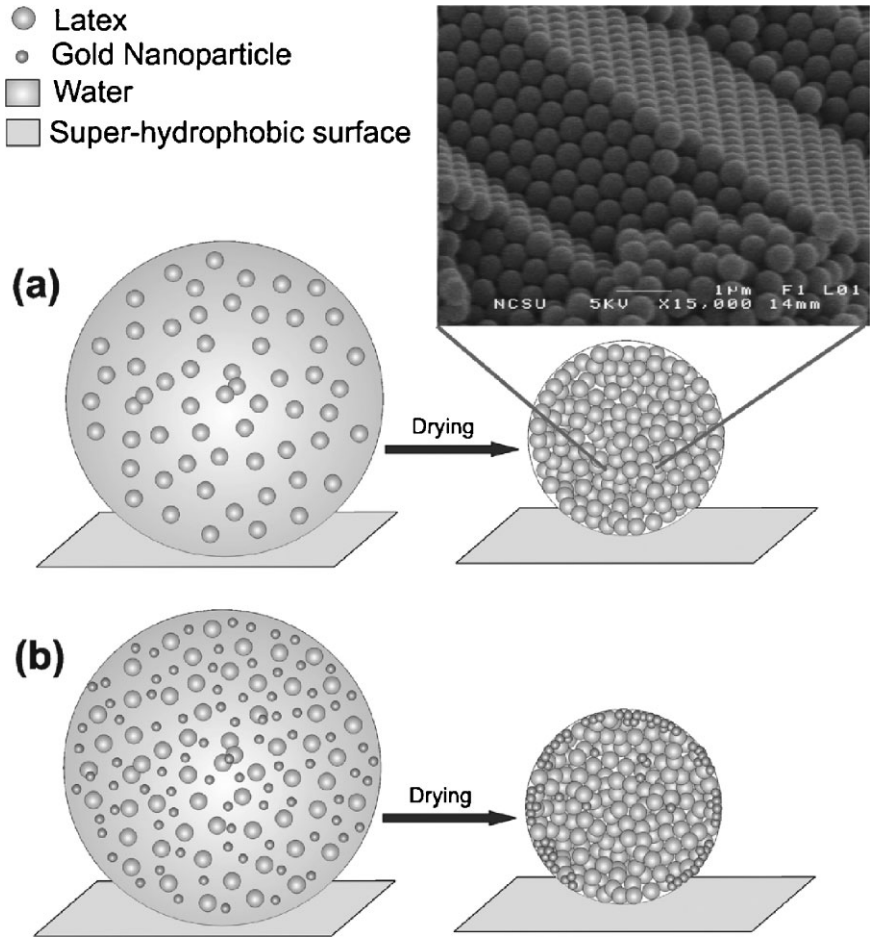

Figure 1. Schematics of the process for making spherical colloidal assemblies on superhydrophobic surfaces: a) latex opal ball, and b) latex and gold opal ball. The inset is a scanning electron microscopy image that displays the hexagonal close-packed structure of latex spheres inside an opal ball of 540 nm latex.

The droplet templates easily roll off Si-NW substrates owing to their extremely high hydrophobicity and low contact-angle hysteresis. Hence, artificial local pinning spots were created by scratching with a sharp needle on such substrates to anchor the droplet templates. We did not encounter this problem while working with LDPE substrates because of the measurable difference between their advancing and receding contact angles.[41] The cracks between the LDPE crystals on the substrate act as small pinning areas. These areas were used to hold the droplets in place while letting them dry. The free volume available for the latex particles in the water droplets keeps decreasing because of solvent evaporation, hence, the particles are forced to organize into close-packed microsphere crystals (inset of Fig. 1a). The droplets were continuously monitored during the drying process while illuminated with a near-collimated beam of light. The surface of the drying droplets begins to display colored ringlike diffraction patterns within 15 min of dispensing the droplets. The colored rings appear because of the formation of colloidal crystals from latex spheres adjacent to the surface by concentration of the particles left behind by the evaporating water. A typical timeline of appearance of colored ring patterns in suspended droplets with latex spheres is presented in Figure 2a. We refer to these structures as ''opal balls'' because of their colorful appearance. After ca. 60 min almost all of the solvent has evaporated and a supraball with a hexagonal close-packed crystal arrangement of polystyrene spheres is formed (inset in Fig. 1a). We dispensed multiple droplets on the same substrate and studied the shape of the final dried supraballs by imaging their top and side profiles. Their structure and resulting diffraction pattern are analyzed and discussed in the later part of this Communication.

In the next step of the experiments, we prepared supraparticles from a mixed suspension of latex microspheres and gold nanoparticles. Because the gold nanoparticles are small enough to pass through the interstices of the latex particles, most of them are transported to the surface during the solvent evaporation. Thus, the concentration of gold nanoparticles near the supraparticle surface increases over time. During the final stages of drying, the gold nanoparticle suspension dewets the latex microsphere network and clusters within some of the crystal domains on the supraparticle surface. Continuous monitoring by high-magnification optical microscopy and scanning electron microscopy (SEM) analysis of dried supraparticle surfaces (Fig. 3) provide evidence for the dewetting phenomena. The results point out that during the co-assembly process the gold nanoparticle aggregates are deposited in and around the voids in the latex crystal network without altering the packing density of the latex spheres in the supraballs. The gold nanoparticle network does not change the structure or cover completely the latex crystal domains on the supraball surface, which retain a similar colored ring appearance as in the latex-only supraballs. The microsphere arrangement was analyzed by comparing scanning electron microscopy images of latex opal balls (inset Fig. 1a) with latex and gold opal balls (Fig. 3). The presence of gold nanoparticles aids in observing high-contrast colors on the surface of the assemblies (Fig. 2b and c).

A notable feature of these assemblies is that they sparkle in a multitude of colors. The colored domains are organized in series of concentric rings. The surface of the opal balls is made from localized crystal domains, which diffract light in different directions depending on the relative orientation of their crystal plane with respect to a fixed-position light source and the opal

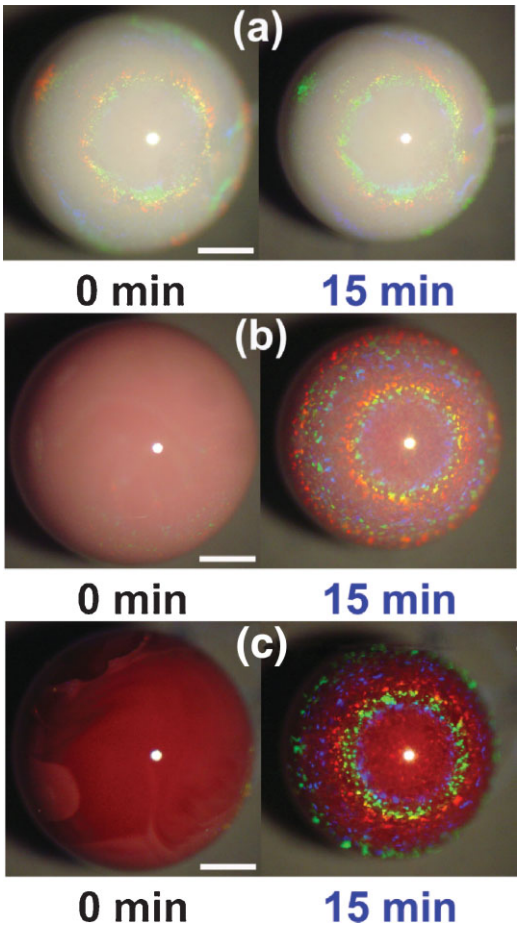

Figure 2. Timeline of formation of spherical opal assemblies on a superhydrophobic Si-NW substrate: a) latex, b) latex and 0.1 wt % Au nanoparticles, and c) latex and 1.0 wt % Au nanoparticles. The latex microsphere diameter is 540 nm in each droplet. The Au nanoparticle diameter is 22 nm. Scale bars: 500 μm.

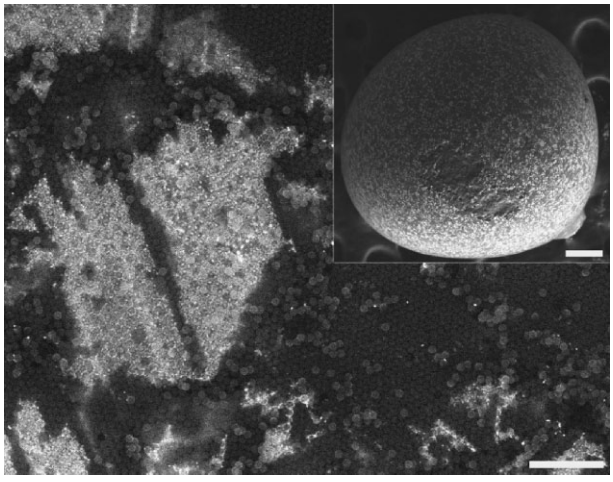

Figure 3. SEM image of the surface of a supraparticle made from a mixture of 540 nm latex and 22 nm gold nanoparticles. Dark spheres are latex and bright regions are clusters of gold nanoparticles. Scale bar: 5 μm. The inset is a SEM image of the whole supraparticle with patches of gold scattered all over the surface. The scale bar in the inset is 200 μm.

ball. That is why the rings appear fragmented in domains of slightly different colors. We used different size latex particles to determine how their diameter affects both the size and color of the diffraction rings on the surface of the supraballs. The diameters of the latex particles were 320 nm, 420 nm, 540 nm, 720 nm, 810 nm, and 1000 nm (Fig. 4). These latex suspensions were also mixed with 0.21 wt % colloidal gold suspension in 1:1 volumetric ratio to make latex and gold opal balls (Fig. 5). The gold suspension dilutes the latex particles suspension by 50%, and thus the supraballs in Figure 5 are smaller than the ones in Figure 4. We observe reductions in the sizes of the colored rings on the supraball surface as the diameter of latex microspheres is increased from 420 nm to 1000 nm. The number of rings also increases with increasing latex diameter. The supraballs from 320 nm latex particles exhibit only one blue ring (Figs. 4 and 5), while supraballs with higher latex diameters produce blue, green, yellow, and red rings.

We investigated the physical origin of the colored rings and their correlation with the microsphere diameter and size of the supraballs. The commonly reported Bragg diffraction from in-depth parallel layers of colloidal crystals does not explain our experimental results. Instead, we considered how the rows of particles on the surface of the supraballs interact with the incident light to render Bragg-type diffraction pattern. The interparticle spacing on the surface is varied by changing the size of the latex particles, which is analogous to changing the groove density in a diffraction grating. Light waves reflected from two adjacent "grooves" (particle lines) on the supraparticle surface undergo constructive or destructive interference, depending on the path difference. The diffraction–reflection phenomenon occurs solely on the surface so the effective refractive index of the media is the same as air. The following formula for the path difference was derived from the geometry of the curved supraparticle surface (Fig. 6)

$$m\lambda = d \times [\sin(90 - \alpha) + \sin(\theta - \alpha)] \quad (1)$$

where $m = 1, 2, 3 \ldots$ for first, second, and third sets of rings, respectively. The wavelength, λ, of the specific spot on a colored ring is estimated by comparing circular spots of 10 pixel diameter from the colored rings in the optical micrograph of the opal ball to the standard Commission internationale de l'éclairage (CIE) 1931 chromaticity diagram.[42] The variable d is the interplanar spacing for the colloidal crystal. The latex particles in the opal balls are arranged in the form of a face-centered cubic (FCC) lattice with the (111) plane parallel to the outer interface.[43] The interplanar spacing for (111) planes is $d = \sqrt{2/3}D$[44] (D is the diameter of latex particles). θ is the angle between the incident beam direction and the horizontal plane (Fig. 6). The calculations for θ were done using two different geometrical methods. The first method takes into account the position of the shadow edge relative to the geometrical center of the supraparticle in the optical microscopy image. Height and distance trigonometry formulae were applied using measurements from side and top profile images

ADVANCED MATERIALS

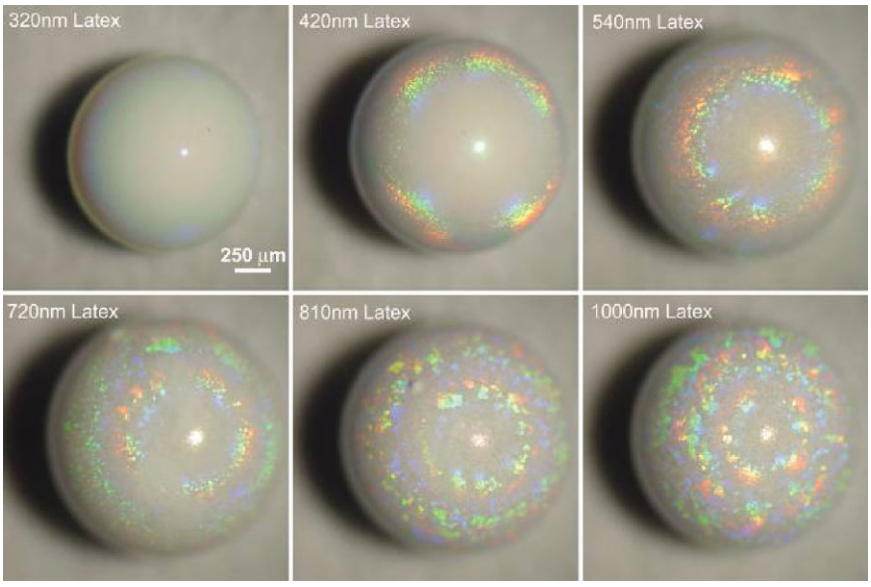

Figure 4. Optical microscopy images of latex opal balls made from microspheres with varying sizes taken under identical illumination conditions.

of the opal balls for determining θ. We also estimated θ from the relative position of the illuminator spot with respect to the geometric center of the supraparticle. The values of θ obtained from both methods agree well with each other. For the images analyzed here, θ takes a value close to 66°. The angle α (between the radial direction and the horizontal plane) is calculated using the position of the colored spot under consideration relative to the center of the supraball.

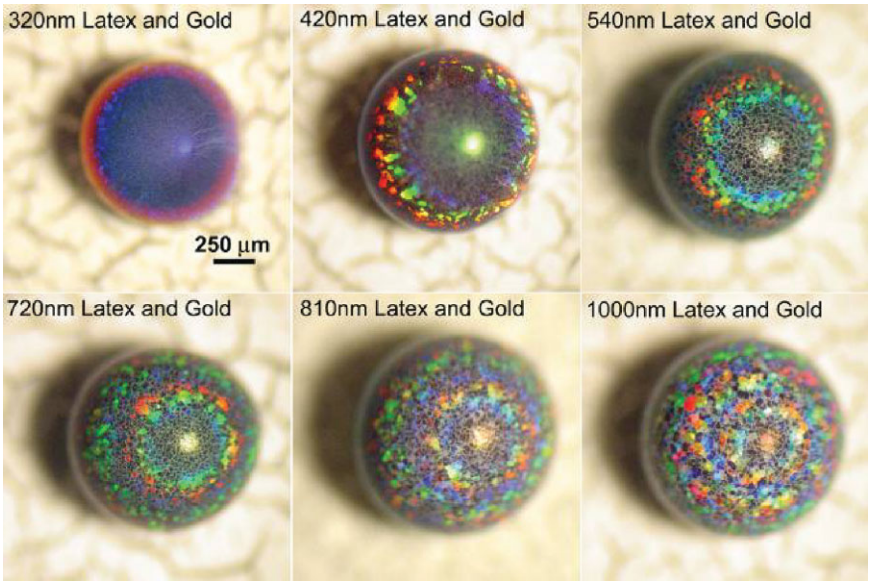

Figure 5. Optical microscopy images of latex and gold nanoparticle opal balls containing microspheres of varying sizes, as in Figure 4.

A qualitative inspection of Equation 1 allows us to arrive at the following conclusions in agreement with the experimental observations (see Fig. 4): First, as we move further away from the position of the illuminator spot (which corresponds to $m = 0$, that is $\alpha - \theta = 90° - \alpha$) along the supraball surface, the path difference increases and, thus, shorter-wavelength rings will appear closer to the illuminator spot. Second, an increase of latex particle size will lead to smaller diameter rings because the path difference should decrease proportionally to particle size. Note that the angular position of the rings (determined by α) will not be affected by the overall size of the opal balls. Opal balls with different sizes formed by latex particles of equal diameters will show the same pattern of diffraction rings. Indeed, identical colored ring patterns were formed in the experiment in supraballs of varying sizes synthesized from same diameter latex. The number of rings and their angular positions (determined by α) in each supraball was similar regardless of their overall size, satisfying the conditions for same α values in Equation 1.

The numerical measurements of the reflected wavelengths allowed us to compare our experimental results with Equation 1 in a more quantitative way. In Figure 7 we plot the variation of the normalized path length $[\sin(90 - \alpha) + \sin(\theta - \alpha)]$ with respect to the normalized wavelength $m\lambda/d$ for latex opal balls without Au nanoparticles. The experimental data follow a linear trend as predicted by Equation 1, without the use of any fitting parameter (Fig. 7). All data points are scattered close to the $y = x$ line, which corresponds well with our theoretical estimates. This indicates that the colors of the rings of the supraparticles arise from surface light diffraction and are independent of the internal structure.

The same type of optical analysis was done for the diffraction properties of latex and gold nanoparticle supraballs. The data for latex and gold nanoparticle balls match very well the diffraction grating theory in the same fashion as the latex opal balls (Fig. 7). The colored rings in latex and gold opal balls have exactly the same functional dependence on microsphere diameter and supraparticle size as the latex opal balls. This points out that the plasmon resonance of the gold nanoparticles on the surface does not

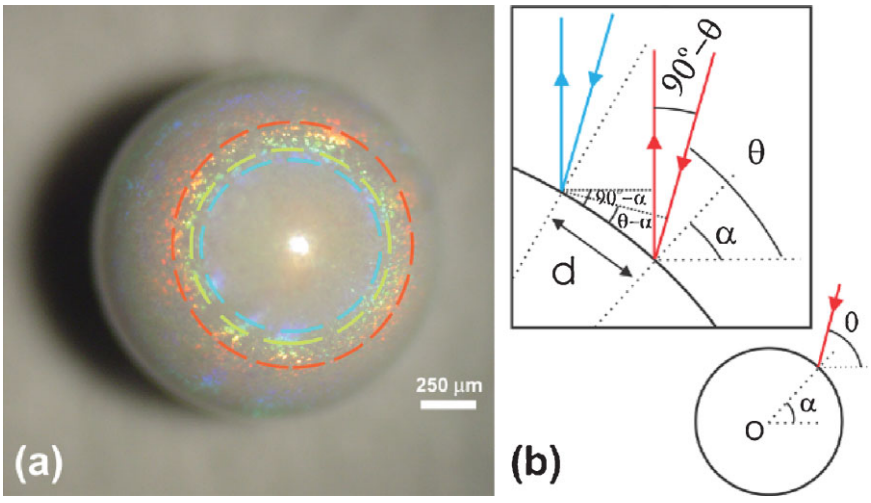

Figure 6. a) Colored rings in the top-view of a 540 nm latex opal ball. b) Side-view schematics of the angles used in the theoretical calculation of wavelength for a particular color ring.

affect the formation of the colored rings and corroborates our previous conclusion that the interparticle spacing in the latex crystal does not change in the presence of the Au nanoparticles. The presence of gold nanoparticles in the pores between the latex, however, attenuates the back-scattering of light from the bulk, leading to the blackish appearance of latex and gold opal balls. This unexpected result also proves in another way our assumption that there is no contribution from bulk scattering inside the supraparticles in the development of colored rings. The nanoparticles simply enhance the visual attractiveness of the supraparticles by providing a dark background to create a better contrast for sharper visibility of the colored rings.

The method reported here is extremely easy to implement and avoids the oil-removal step,[29] thus making the colloidal assemblies ready to collect and use. They can be easily detached from the substrate by gently tapping on the bottom of the superhydrophobic substrate. The dried spherical particle assemblies sometimes have a small flat area on the bottom due to the initial pinning of droplet templates. A detailed analysis of the evolution of the droplet shape is beyond the scope of this Communication. A substrate with a higher degree of hydrophobicity and lower difference between advancing and receding contact angles can reduce the pinning area, thus minimizing deviation from spherical shape in colloidal particles assemblies. However, this poses the problem of holding the droplets in place during manual dispensing. One solution could be to use ink-jet printing to dispense the droplets on a substrate with predefined pinning spots of minimal dimensions. The production of supraballs can be easily automated by continuous dispensing of droplets on one side of a LDPE-crystal-coated ''conveyor belt'', and collecting dried assemblies on the other side.

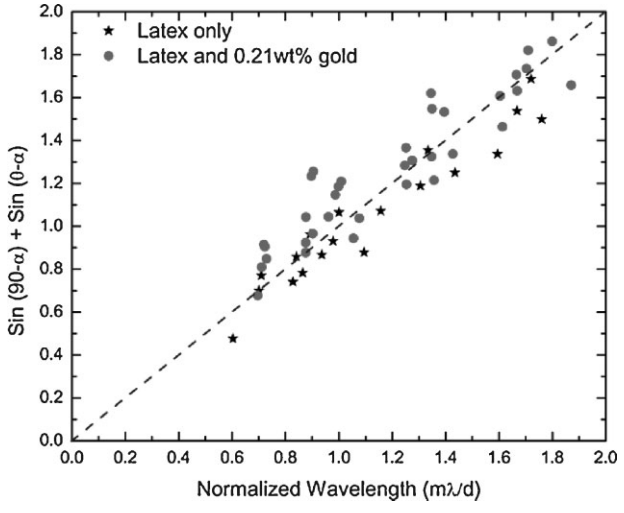

Figure 7. Normalized path difference versus the normalized wavelength for colored ring patterns in latex opal balls and latex/gold opal balls.

The opal balls do not disintegrate when exposed to water. The near-spherical shape allows creation of discrete color bands upon exposure to collimated white light. Such particles can be used in decorative coatings. The well-defined and uniform pore size of the supraparticles can be used in applications such as drug delivery to provide slow controlled-rate release of an infused drug. The conjugation of the microsphere surface with enzymes before forming supraparticles or including live cells within the structure can be utilized in the preparation of biocatalytic supports.[29] Magnetic functionality can be introduced in latex opal balls by adding magnetic nanoparticles to the initial latex suspension. We showed that nonuniform magnetic fields can pull the magnetic microparticles into the top hemisphere. Such anisotropic magnetic particles can be easily rotated and used, for example, for mixing in microfluidic devices. The methods and the types of supraballs formed can be diversified much in future research. The supraballs that we assembled to date are of millimeter-scale diameter. Depending on the precision in metering of initial droplet volume and local substrate properties, supraballs produced in the same batch had a variation of 10% in shape and size. Further refinements are required for control of the final size of the supraparticles. Owing to their close-packed structure, the latex spheres have maximum contact with their neighboring particles. However, the supraparticles still manifest brittleness because of the low strength of van der Waals attractions at small contact areas between microspheres. This creates the need for further reinforcement procedures to increase the mechanical stability of the structures.

In summary we demonstrate here a simple yet powerful technique that can be used in massively parallel manufacturing of diffracting particle assemblies in droplets suspended on

ADVANCED MATERIALS

superhydrophobic substrates. The reflection bands in the ''opal balls'' originate from diffraction by the parallel crystal rows on the surface, instead of bulk Bragg scattering. The presence of metallic nanoparticles in the structure does not lead to a shift of the reflection band by plasmon resonance, but enhances the diffraction color by increased reflectance and suppressed backscattering. The uniform supraballs can find application in photonics, drug delivery, special coatings, sensors, and microfluidics.

Experimental

Surfactant-free, sulfate-stabilized polystyrene latex microspheres were purchased from Interfacial Dynamics Corp. (Portland, OR, USA). Deionized (DI) water was obtained from Millipore RiOs 16 reverse-osmosis water purification systems (Bedford, MA, USA). 20 vol % latex particle suspensions in water were prepared by washing the latex particles twice with DI water and centrifuging them at 3000 *g* for 20 min. After decanting the supernatant, the latex particles were sonicated and mixed with DI water to obtain the desired volume fraction. The gold nanoparticles used for doping of the latex opal balls were synthesized by reduction of $HAuCl_4$ with sodium citrate and tannic acid, which yielded suspensions of ca. 22 nm gold nanoparticles [45]. All chemicals were used as-purchased from Fisher (Pittsburgh, PA) or Aldrich (Milwaukee, WI). The nanoparticle suspensions were concentrated 100-fold via centrifugation (1500 *g* for 10 min) in Millipore Biomax 5 centrifuge filters. Residual salts were washed by centrifuging DI water through the filters (1500 *g* for 10 min). The gold nanoparticles were further concentrated by another 10-fold by using a Marathon micro A microcentrifuge at 8500 g for 15 min. The final concentration of gold nanoparticles in the water suspensions studied was approx. 0.21 wt %. The precise nanoparticle concentrations were measured by UV-vis spectrophotometry at the gold nanoparticle surface plasmon resonance (SPR) peak. The position of the SPR peak for all samples remained constant at (522 ± 1) nm, which is consistent with stable, unaggregated suspensions of 20–22 nm sized particles [46]. The latex suspension was mixed in 1:1 volume ratio with 0.21 wt % gold nanoparticle suspension.

5.0 μL droplets containing the suspension of microspheres and gold nanoparticles were dispensed onto the superhydrophobic substrate using an ultra-micropipette (Eppendorf North America Inc., NY, USA). The droplets were allowed to dry at ambient temperature ((22 ± 1) °C) in a dry environment created using desiccant. Microseparation of particles resulting from evaporation in the droplets was monitored from the top using a SZ61 (0.7–4.5× zoom) stereomicroscope (Olympus America Inc., NY, USA). Images were captured at regular intervals using DSC-V1 Cyber-Shot digital camera (SONY, Japan) coupled with the microscope.

Received: December 3, 2007
Revised: February 17, 2008
Published online: July 28, 2008

[1] A. van Blaaderen, *MRS Bull.* **1998**, *23*, 39.
[2] V. L. Colvin, *MRS Bull.* **2001**, *26*, 637.
[3] R. Rengarajan, P. Jiang, D. C. Larrabee, V. L. Colvin, D. M. Mittleman, *Phys. Rev. B* **2001**, *6420.*
[4] C. Lopez, *J. Opt. A* **2006**, *8*, R1.
[5] G. Subramania, K. Constant, R. Biswas, M. M. Sigalas, K. M. Ho, *Appl. Phys. Lett.* **1999**, *74*, 3933.
[6] Y. A. Vlasov, V. N. Astratov, O. Z. Karimov, A. A. Kaplyanskii, V. N. Bogomolov, A. V. Prokofiev, *Phys. Rev. B* **1997**, *55*, 13357.
[7] J. D. Joannopoulos, P. R. Villeneuve, S. Fan, *Nature* **1997**, *386*, 143.
[8] D. J. Norris, *Nat. Mater.* **2007**, *6*, 177.
[9] Y. Lu, Y. Yin, Y. Xia, *Adv. Mater.* **2001**, *13*, 415.
[10] F. Meseguer, *Colloids Surf. A* **2005**, *270–271*, 1.
[11] P. V. Braun, S. A. Rinne, F. García-Santamaría, *Adv. Mater.* **2006**, *18*, 2665.
[12] A.-P. Hynninen, J. H. J. Thijssen, E. C. M. Vermolen, M. Dijkstra, A. van Blaaderen, *Nat. Mater.* **2007**, *6*, 202.
[13] Y. Xia, B. Gates, Z.-Y. Li, *Adv. Mater.* **2001**, *13*, 409.
[14] A. van Blaaderen, *Science* **1998**, *282*, 887.
[15] F. García-Santamaría, J. F. Galisteo-Lopez, P. V. Braun, C. Lopez, *Phys. Rev. B* **2005**, *71.*
[16] H. Fudouzi, Y. N. Xia, *Langmuir* **2003**, *19*, 9653.
[17] B. Gates, Y. Lu, Z. Y. Li, Y. Xia, *Appl. Phys. A* **2003**, *76*, 509.
[18] S. I. Matsushita, Y. Yagi, T. Miwa, D. A. Tryk, T. Koda, A. Fujishima, *Langmuir* **2000**, *16*, 636.
[19] B. G. Prevo, J. C. Fuller, O. D. Velev, *Chem. Mater.* **2005**, *17*, 28.
[20] B. G. Prevo, E. W. Hon, O. D. Velev, *J. Mater. Chem.* **2007**, *17*, 791.
[21] K. Burkert, T. Neumann, J. J. Wang, U. Jonas, W. Knoll, H. Ottleben, *Langmuir* **2007**, *23*, 3478.
[22] V. Rastogi, O. D. Velev, *Biomicrofluidics* **2007**, *1*, 014107.
[23] A. Cho, *Science* **2003**, *299*, 1684.
[24] D. R. Rolison, *Science* **2003**, *299*, 1698.
[25] J. R. Millman, K. H. Bhatt, B. G. Prevo, O. D. Velev, *Nat. Mater.* **2005**, *4*, 98.
[26] O. D. Velev, A. M. Lenhoff, *Curr. Opin. Colloid Interface Sci.* **2000**, *5*, 56.
[27] A. D. Dinsmore, M. F. Hsu, M. G. Nikolaides, M. Marquez, A. R. Bausch, D. A. Weitz, *Science* **2002**, *298*, 1006.
[28] V. N. Paunov, O. J. Cayre, *Adv. Mater.* **2004**, *16*, 788.
[29] O. D. Velev, A. M. Lenhoff, E. W. Kaler, *Science* **2000**, *287*, 2240.
[30] K. P. Velikov, O. D. Velev, *Colloidal Particles at Liquid Interfaces*, B.P. Binks, T. S. Horozov), University Press, Cambridge, UK **2006**, pp. 225–297.
[31] O. D. Velev, K. Furusawa, K. Nagayama, *Langmuir* **1996**, *12*, 2374.
[32] O. D. Velev, K. Furusawa, K. Nagayama, *Langmuir* **1996**, *12*, 2385.
[33] O. D. Velev, K. Nagayama, *Langmuir* **1997**, *13*, 1856.
[34] V. N. Manoharan, A. Imhof, J. D. Thorne, D. J. Pine, *Adv. Mater.* **2001**, *13*, 447.
[35] S. Melle, M. Lask, G. G. Fuller, *Langmuir* **2005**, *21*, 2158.
[36] S. M. Klein, V. N. Manoharan, D. J. Pine, F. F. Lange, *Langmuir* **2005**, *21*, 6669.
[37] S. H. Kim, S. Y. Lee, G.-R. Yi, D. J. Pine, S.-M. Yang, *J. Am. Chem. Soc.* **2006**, *128*, 10897.
[38] J. Park, J. Moon, H. Shin, D. Wang, M. Park, *J. Colloid Interface Sci.* **2006**, *298*, 713.
[39] D. M. Kuncicky, K. Bose, K. D. Costa, O. D. Velev, *Chem. Mater.* **2007**, *19*, 141.
[40] D. M. Kuncicky, O. D. Velev, *Langmuir* **2008**, *24*, 1371.
[41] A. Egatz-Gómez, J. Schneider, P. Aella, D. Yang, P. Domínguez-García, S. Lindsay, S. T. Picraux, M. A. Rubio, S. Melle, M. Marquez, A. A. García, *Appl. Surf. Sci.* **2007**, *254*, 330.
[42] J. Orava, T. Jääskeläinen, J. Parkkinen, V.-P. Leppanen, *Colloids Res. Appl.* **2007**, *32*, 409.
[43] S.-C. Mau, D. A. Huse, *Phys. Rev. E* **1999**, *59*, 4396 LP.
[44] A. Richel, N. P. Johnson, D. W. McComb, *Appl. Phys. Lett.* **2000**, *76*, 1816.
[45] J. W. Slot, H. J. Geuze, *Eur. J. Cell Biol.* **1985**, *38*, 87.
[46] S. Link, M. A. El-Sayed, *J. Phys. Chem. B* **1999**, *103*, 4212.